ISBN: 978-3-95450-219-6 ISSN: 2226-0366 doi: 10.18429/JACoW-LINAC2024-THPB060

CBXFEL DESIGN, PRODUCTION, AND INSTALLATION STATUS*

M. White†, J. Anton, L. Assoufid, A. Bernhard, D. Bianculli, M. Golebiowski, X. Huang, W. Jansma, A. Karales, K. Kauchha, S. Kearney, K.-J. Kim, K. Lang, R. Lindberg, P. Liu, R. Margraf-O'Neal, M. Martens, S. Mashrafi, A. Miceli, Jeong-Wan Park, P. Pradhan, M. Rivers, X. Shi, D. Shu, Y. Shvyd'ko, J. Sullivan, J. Tijerina, D.A. Walko
Argonne National Laboratory, Lemont, IL, USA
N. Balakrishnan, M. Balcazar, C. Curtis, F.-J. Decker, G. Gassner, A. Halavanau, Z. Huang, B. Jocson, E. Kraft, G. Lanza, A. Lutman, J. Mock, M.A. Montironi, X. Permanyer, S. Saraf, T. Sato, J. Tang, D. Zhu, SLAC National Accelerator Laboratory, Menlo Park, CA, USA
T. Osaka, K. Tamasaku, RIKEN SPring-8 Center, Saitama, Japan
W. Lewis, S.J. Stein, OspreyDCS, Ocean City, MD, USA
M. Camarena, C. Jing, B. Wyderski, Euclid Beamlabs LLC, Bolingbrook, IL, USA

Abstract

Use of a cavity-based X-ray free electron laser (CBXFEL) is potentially a way to dramatically improve the stability and coherence of existing XFELs. A proof-of-principle project is underway as a collaboration between Argonne National Laboratory (ANL), The Institute of Physical and Chemical Research in Japan (RIKEN), and SLAC National Accelerator Laboratory. The CBXFEL is expected to operate using 9.831 keV photons from LCLS, using synthetic diamonds as cavity Bragg mirrors. The LCLS copper linac will deliver two electron bunches 624 RF buckets apart, resulting in a total X-ray cavity length of 65500.87 mm. The X-ray cavity design, and installation and production status will be presented.

EXPERIMENTAL LAYOUT

As shown in Fig. 1, the first seven LCLS hard X-ray undulators are within the optical cavity delineated by the four diamond Bragg-reflecting crystal mirrors C1, C2, C3, and C4. A chicane diverts the incoming electron beam around the crystal mirror C4 in Fig. 1. The electron beam passes through the seven undulators creating x-rays, and continues on to be diverted around the C1 crystal mirror by a second chicane. The design allows for precision alignment of the diamond mirrors using sophisticated nano-positioning systems, such that the produced x-rays can continue to be reflected around the cavity. Stations A & B contain the four diamond crystal mirrors and their nano-positioning systems. Stations C, D, E, F, and G also shown in Fig. 1, host additional X-ray diagnostics.

Diamond Crystal Mirrors

The diamond crystals, grown by Sumitomo under contract to RIKEN, were qualified after extensive testing [1]. Processes were developed to machine and anneal the diamonds for optimal shape and performance. The left side of Fig. 2 shows the results of the process, where strain relief cuts have been machined into the crystal to prevent strain

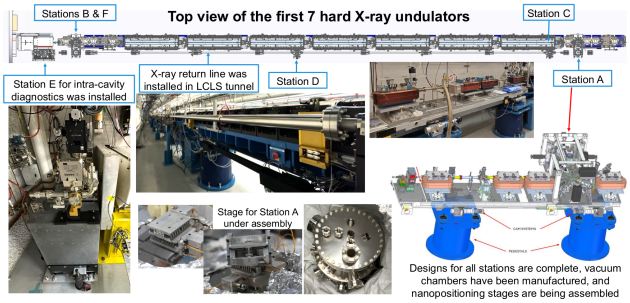

Figure 1: Overview of the CBXFEL cavity, including stations A and B that house the diamond crystals mirrors and beryllium x-ray lenses, chicanes that divert the electron beam around the crystals, X-ray diagnostics stations C, D, E, and F, and the X-ray return line.

from the mounting clamps on the right to affect the working area boxed in red. After high-temperature annealing, X-ray Rocking Curve Imaging (RCI) shows a nearly ideal Darwin width that is nearly constant over a 2 mm^2 working area.

In addition to the usual treatment that is applied to the nearly 100% reflective crystals C2, C3, and C4, thin, "drumhead" membranes were laser-ablated into C1 to allow for outcoupling of ~5% of the X-rays [2]. We show RCI results in Fig. 2 both before (middle top) and after (middle bottom) laser ablation. The bottom shows that while the Darwin width increases somewhat because of the crystal thickness reduction, the center of mass of the reflection is unchanged. This indicates a nearly strain-free membrane whose thickness of ~17 microns results in a measured Rocking curve that agrees very well with ideal simulations as shown on the right of Fig. 2.

Simulations

Extensive simulations were performed to understand the ideal CBXFEL performance, the required mechanical tolerances, and the effects of cavity misalignments. Figure 3 shows the expected 2-bunch gain and source properties obtained from GENESIS simulations. The top row plots the power along the undulator (left), along with the X-ray spectrum generated by the first bunch (middle) and the second

* Work supported by U.S. Department of Energy, Office of Science under contracts DE-AC02-06CH11357 and DE-AC02-76FO0515.
† mwhite@anl.gov

ISBN: 978-3-95450-219-6 ISSN: 2226-0366 doi: 10.18429/JACoW-LINAC2024-THPB060

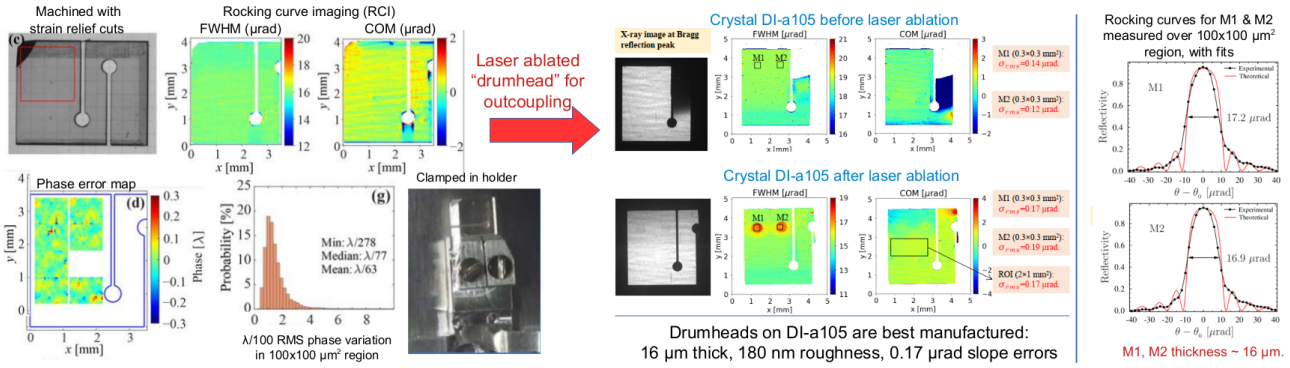

Figure 2: Diamond crystal machining, initial characterization, drumhead ablation, and final characterization including Darwin widths that closely match theory for 17 micron thick outcoupling drumhead.

bunch (right). The FEL gain in the second bunch amplifies the spectral power within the narrow crystal bandwidth by a factor of 50 to 100 over the SASE background, which in turn leads to the significant improvement of transverse coherence shown in the second row of Fig. 3.

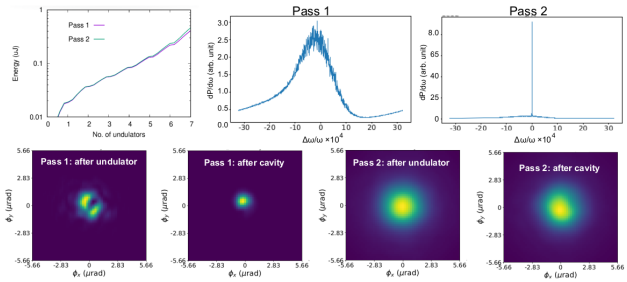

Figure 3: Genesis simulations of CBXFEL showing a gain between 50 and 100 within the narrow crystal bandwidth.

We also simulated various transverse and longitudinal misalignment scenarios to determine tolerances. Maintaining 2-pass gain requires that the timing and position of the second bunch be accurate to better than 50% of the rms sizes, translating to a temporal accuracy of less than 25 fs and transverse misalignments smaller than 10 microns for the case in Fig. 3; the implied crystal stability requirement of better than 50 nrad has been incorporated in the design. Simulation results that show similar angular tolerance requirements during initial alignment [3] are shown on the right side of Fig. 4.

MECHANICAL SYSTEMS

Stations A and B, shown in the upper right corner of Fig. 4, contain the diamond crystal mirrors. Each station is comprised of two separate vacuum chambers housing the nanopositioning systems that support the diamond mirrors and enable their remote angular and spatial alignment and optimization. As shown in the figure, diagnostic Stations C and D are located in the x-ray return line.

All vacuum chambers are fabricated, and internal components are received. Station D is installed at LCLS, together with the drift sections of the x-ray return line. Station C is undergoing final checkout at SLAC and is expected to be installed in LCLS during the November 2024 down period.

Stations A and B are being assembled. Assembly procedures were developed, fiducialization procedures were written and tested, and all procedures are being finalized. Because these chambers are directly tied into the accelerator vacuum, the vacuum requirements are extremely stringent. A photograph of one of the diamond-mirror-containing chambers is shown in Fig. 1.

X-RAY OPTICS AND DIAGNOSTICS

X-ray optics return a nearly monochromatic and focused X-ray beam for subsequent amplification. We already discussed the four Bragg-reflecting diamond crystal mirrors that reflect a narrow-band signal at 45 degrees. The cavity also houses two beryllium refractive x-ray lenses just after C1 and C3, which control the transverse x-ray beam profile. These were characterized at the APS, showing that they will provide a 23 m focal length with very small wavefront phase errors.

X-ray diagnostics are another critical part of the project, providing the means to align the cavity, monitor its status, and measure the final output [4]. The top of Fig. 4 shows the planned layout of the x-ray diagnostic suite within the cavity. X-ray beam position monitors (BPMs) are shown as yellow and blue rectangles, and are located before and after each crystal to help direct the x-ray beam to the subsequent crystal. Photodiodes are positioned behind crystals C2, C3, and C4 where the x-ray signal is nearly monochromatic. By minimizing the transmitted x-ray signal through the crystals, we can accurately match the crystal angle to the 45 degree Bragg angle. The layout in Fig. 4 also shows the grating in station D that will direct ~10% of the x-rays to station E where detailed information including the x-ray wavefront within the cavity can be measured.

The lower left of Fig. 4 also shows an example of the expected signal from the beam overlap diagnostic located in station F. Test results from the fast YAP screen are also plotted, along with some examples of the diamond XBPMs. The right-most plots in Fig. 4 show examples of ray-tracing simulations of the entire diagnostic suite, showing how various crystal misalignment angles can be detected in the diodes.

ISBN: 978-3-95450-219-6 ISSN: 2226-0366 doi: 10.18429/JACoW-LINAC2024-THPB060

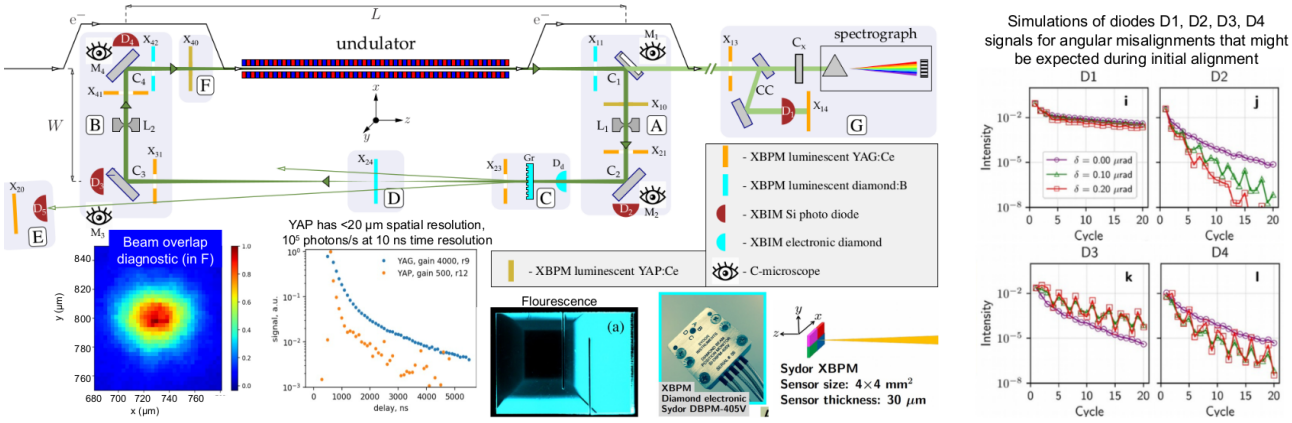

Figure 4: Layout of the X-ray diagnostic design with examples of test results. Far right shows simulation results of the diode measurements for various cavity misalignments [3].

ACCELERATOR PREPARATION

There has been significant progress in preparing the LCLS accelerator for CBXFEL. First, new, fast transverse kickers were installed to separately control the transverse orbit of both bunches and insure that they align with each other in both position and angle. Next, we have used the hard X-ray self seeding system to verify the expected gain over the seven undulators. We show examples of such measurements in Fig. 5. The left panel plots the FEL gain as a function of the number of undulators, and shows a ~3 m gain length and approximately 720 nJ of X-ray energy after 7 undulators. The right panel shows the a number of measured FEL spectra after the self-seeding monochromator. We see that even after 5 hard x-ray undulators (HXUs) there is a measurable signal, while 7 HXUs show a significant narrow-bandwidth signal that we can expect from CBXFEL.

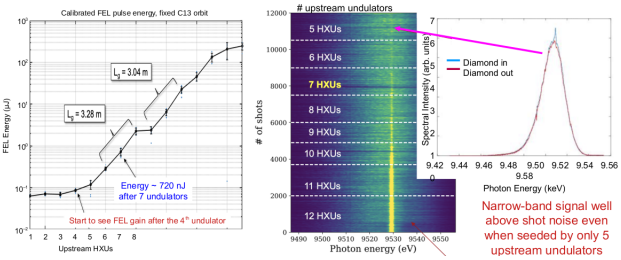

Figure 5: Measurements of the LCLS FEL gain and seeding performance.

CONTROLS

A sophisticated motion control system is responsible for positioning the diamond mirrors within the CBXFEL chambers. Each of the four major chambers (C1, C2, C3, C4) contains a stack of high-precision flexure stages driven by Newport Picomotors [5], with absolute position measured by aligned capacitive sensors from Lion Technologies [6]. Two stages move the mirror linearly, while the other two control pitch and roll angles relative to the beam axis. Coarse linear motion for initial alignment of the diamond mirror uses small, in-vacuum linear stages from SmarAct [7]. The pitch and roll stages incorporate fine adjustment via a closed-loop piezo motor system from PI [8], allowing sub-micron and nano-radian adjustment of the diamond mirror. Feedback for the fine motion is supplied by a commercial dual-head interferometer system from QuTools [9]. All precision motion (Picomotors and piezo motors) is controlled using PowerPMAC [10] control hardware. Picomotors are driven with pulse and direction signals, while piezo motors are driven via an analog signal. Position encoder readback is done via proportional analog signals from the capacitive sensors, and A-Quad-B differential signals for the interferometer. The SmarAct stages are controlled by a separate controller. High-level software includes EPICS databases and control screens for engineering and tuning, as well as for operations and experiments.

CONCLUSIONS

The CBXFEL experiment is in the final stages of assembly and installation; installation and checkout are planned to be completed by July 2025, followed by startup of the experimental program including measurement of ring-down and amplification.

REFERENCES

[1] P. Liu *et al.*, "X-ray optics for the cavity-based X-ray free-electron laser", *J. Synchrotron Radiat.*, vol. 31, no. 4, pp. 751–762, 2024. doi:10.1107/s1600577524003977

[2] P. Pradhan, S. Antipov, and Y. Shvyd'ko, "Fabrication of ultra-thin single crystal diamond membrane by using laser ablation", in *Proc. 2022 SPIE Optical Engineering & Applications*, vol. 12240, San Diego, CA, USA, Aug. 2022, p. 122400A. doi:10.1117/12.2633773

[3] P. Qi and Y. Shvyd'ko, "Signatures of misalignments in X-ray cavities of CBXFELs", *Phys. Rev. Accel. Beams*, vol. 25, p. 050701, 2022. doi:10.1103/physrevaccelbeams.25.050701

[4] P. Liu *et al.*, "X-ray diagnostics for the cavity-based X-ray free-electron laser", *Phys. Rev. Accel. Beams*, to be published.

ISBN: 978-3-95450-219-6 ISSN: 2226-0366 doi: 10.18429/JACoW-LINAC2024-THPB060

[5] Newport Corporation, https://www.newport.com
[6] Lion Precision, https://www.lionprecision.com/.
[7] SmarAct GmBH, https://www.smaract.com/en/.
[8] Physik Instrumente, https://www.pi-usa.us/en/.
[9] qutools GmBH, https://qutools.com/qudis/.
[10] Omron Automation, https://automation.omron.com/en/ca/products/family/pmac%20ide